ATMOSPHERIC SCIENCE

Population dynamics modify urban residents' exposure to extreme temperatures across the United States

Jiachuan Yang[1]*[†], Leiqiu Hu[2]*[†], Chenghao Wang[3]

Exposure to extreme temperatures is one primary cause of weather-related human mortality and morbidity. Global climate change raises the concern of public health under future extreme events, yet spatiotemporal population dynamics have been long overlooked in health risk assessments. Here, we show that the diurnal intra-urban movement alters residents' exposure to extreme temperatures during cold and heat waves. To do so, we incorporate weather simulations with commute-adjusted population profiles over 16 major U.S. metropolitan areas. Urban residents' exposure to heat waves is intensified by 1.9° ± 0.7°C (mean ± SD among cities), and their exposure to cold waves is attenuated by 0.6° ± 0.8°C. The higher than expected exposure to heat waves significantly correlates with the spatial temperature variability and requires serious attention. The essential role of population dynamics should be emphasized in temperature-related climate adaptation strategies for effective and successful interventions.

INTRODUCTION

Extreme heat and cold weather have proved deadly to global residents (1–5). Adaptation to climate extremes becomes increasingly important for urban areas, as cities are and will continue to be the major habitat of global population (6, 7). The ambient temperature–mortality relations in cities often have U- or J-shaped profiles and suggest rapid increases in mortality at extreme temperatures (8, 9). In the context of climatic change, these relations lead to growing concerns about heat-related mortality (10, 11), as heat waves are projected to be more frequent under the warming globe (12). Existing studies on mortality risk commonly use time series of temperature data aggregated over the entire city/region (13–15), with the assumption that the temporal temperature variability can appropriately pick up the risk signal under extreme events. The heterogeneous built-up landscape, nevertheless, causes substantial spatial temperature variations under the same meteorological forcing, where the urban-rural temperature difference can reach more than 10°C across a metropolitan area (16). Furthermore, individual urban agglomerations respond differently to extreme heat and cold (17, 18), e.g., heat islands can intensify extreme urban heat under future heat waves by 2.1° to 4.6°C (19). Robust assessment of residents' mortality risk linked to climate change should therefore account for both spatial and temporal variabilities of temperatures in the complex urban environment.

In light of estimating residents' exposure to extreme temperatures, the spatiotemporal distribution of urban population is equally important as the temperature variability. Recent analysis found that migration patterns at the continental scale could substantially alter U.S. residents' exposure to future extreme heat (20). Within the complex urban environment, the concurrent variations of ambient temperature and population distribution can largely modify individuals' exposure. The modification becomes critical during extreme events, as a 1° or 2°C change in temperature can be consequential for human mortality (21). Work-related commutes can notably increase the daytime urban population in large metropolitan areas, for example, by 95% in New York County, NY (22). Despite the large diurnal population variation, the effect of intra-urban spatiotemporal population dynamics on mortality risk has rarely been studied. The classic temperature-mortality relations, assuming all residents have identical exposures to the mean temperature of each city, are still generally adopted in risk assessment studies (6, 23). One pioneering study looking into temperature-population interactions in Chicago suggested that residents' heat exposure was more responsive to nighttime temperatures during heat waves (24). Whether these findings are generalizable for other metropolitan areas with distinct geoclimatic conditions and landscape features remains unknown.

This study provides the first attempt to quantify urban residents' exposure to heat and cold extremes with a full consideration of spatiotemporal variability of both temperature and population at the intra-urban and subdaily scale. We first estimate residents' exposure temperature simply as the spatial average temperature from weather model simulations over the entire metropolitan areas (hereafter, T_{area}). Then, via incorporating spatiotemporal patterns of commute-adjusted population distribution from transportation census, we obtain new estimates of exposure temperature accounting for population dynamics (hereafter, T_{pop}). Through the comparison of these two exposure temperatures over 16 major urban habitats (table S1) across the contiguous United States (CONUS), we aim to address three questions: (i) To what extent will population dynamics alter urban dwellers' exposure to extreme heat and cold? (ii) How does this modified exposure vary among metropolitan areas? (iii) What are the related variables that contribute to this change? The objective is to measure the impact of population dynamics and to improve the assessment of exposure temperature under heat and cold waves. Examining residents' exposure under future climate scenarios is undoubtedly important; nevertheless, we focus on historical extreme events here to minimize the uncertainty related to climate change and population projections. The lessons learned from the present-day weather hazards are expected to be applicable to future extreme events.

[1]Department of Civil and Environmental Engineering, The Hong Kong University of Science and Technology, Kowloon, Hong Kong, China. [2]Department of Atmospheric and Earth Science, The University of Alabama in Huntsville, Huntsville, AL 35805, USA. [3]School of Sustainable Engineering and the Built Environment, Arizona State University, Tempe, AZ 85287, USA.
*Corresponding author. Email: cejcyang@ust.hk (J.Y.); leiqiu.hu@uah.edu (L.H.)
†These authors contributed equally to this work.

RESULTS

Temperature anomalies during extreme weather

Here, we analyzed the extreme temperature exposure in three massive heat waves and one cold wave (see Materials and Methods). Heat and cold waves create remarkable temperature anomalies across the studied metropolitan areas (fig. S1). In terms of the physical hazard itself, without considering population dynamics, the simulated 2014 cold wave lowers the exposure temperature over the entire metropolitan area (area-weighted daily mean 2-m air temperature, T_{area}) by 11.5° ± 3.2°C (mean ± SD among 12 affected cities), resulting in a mean nighttime T_{area} of −9.1°C over affected cities. The Great Lakes region—including Chicago, Indianapolis, and Columbus—is at the greatest risk with nighttime T_{area} below −18°C (table S2). The mean anomaly under three simulated heat waves (3.6° ± 1.8°C, mean ± SD) is discernible but much smaller than the cold anomaly, with a distinct spatial pattern at the continental scale. Seattle and Los Angeles observe the largest increase of more than 7°C on the west coast (fig. S1); these strong anomalies are partially due to the relatively mild temperatures during normal summer days in coastal cities and the small number of days under the extreme events (table S3).

Impact of population dynamics on exposure temperature

The exposure temperature of urban residents incorporating population dynamics (T_{pop}) is obtained by weighting local hourly 2-m air temperatures by their corresponding population over the entire metropolitan area and then averaging over the diurnal cycle. We considered surrounding suburban zones to cover the full spatial extent of urban residents' daily commute (fig. S2). The impact of spatiotemporal population dynamics, characterized as the difference between exposure temperatures with and without population dynamics ($T_{pop} - T_{area}$), lessens the exposure of urban residents to extreme low temperatures in most cities during the 2014 cold wave (positive values in Fig. 1). Population dynamics are found to have similar effects in normal days (0.6° ± 0.7°C; Fig. 1A) and under the cold wave (0.6° ± 0.8°C; Fig. 1C), with the maximum attenuation effect of more than 1°C found in Albuquerque and Denver. During studied extreme heat events, population dynamics substantially increased urban residents' exposure temperature overall. Compared to T_{area}, T_{pop} is 1.9° ± 0.7°C higher over 16 affected metropolitan regions, where the discrepancy reached up to 3.8°C in Salt Lake City (Fig. 1D). Despite the smaller temperature anomaly posed by heat waves than by the cold wave, the larger difference between T_{pop} and T_{area} suggests the greater role of daily commute in determining total residents' exposure to extreme heat. More residents consistently experience higher than expected temperature under three simulated heat waves, and the discrepancy of this exacerbation among different metropolitan areas under heat waves is more evident than that during the cold wave.

As residents travel to urban cores during daytime and return to residential areas at night (fig. S2), we include a large studied domain including both urban and rural areas for estimating exposure
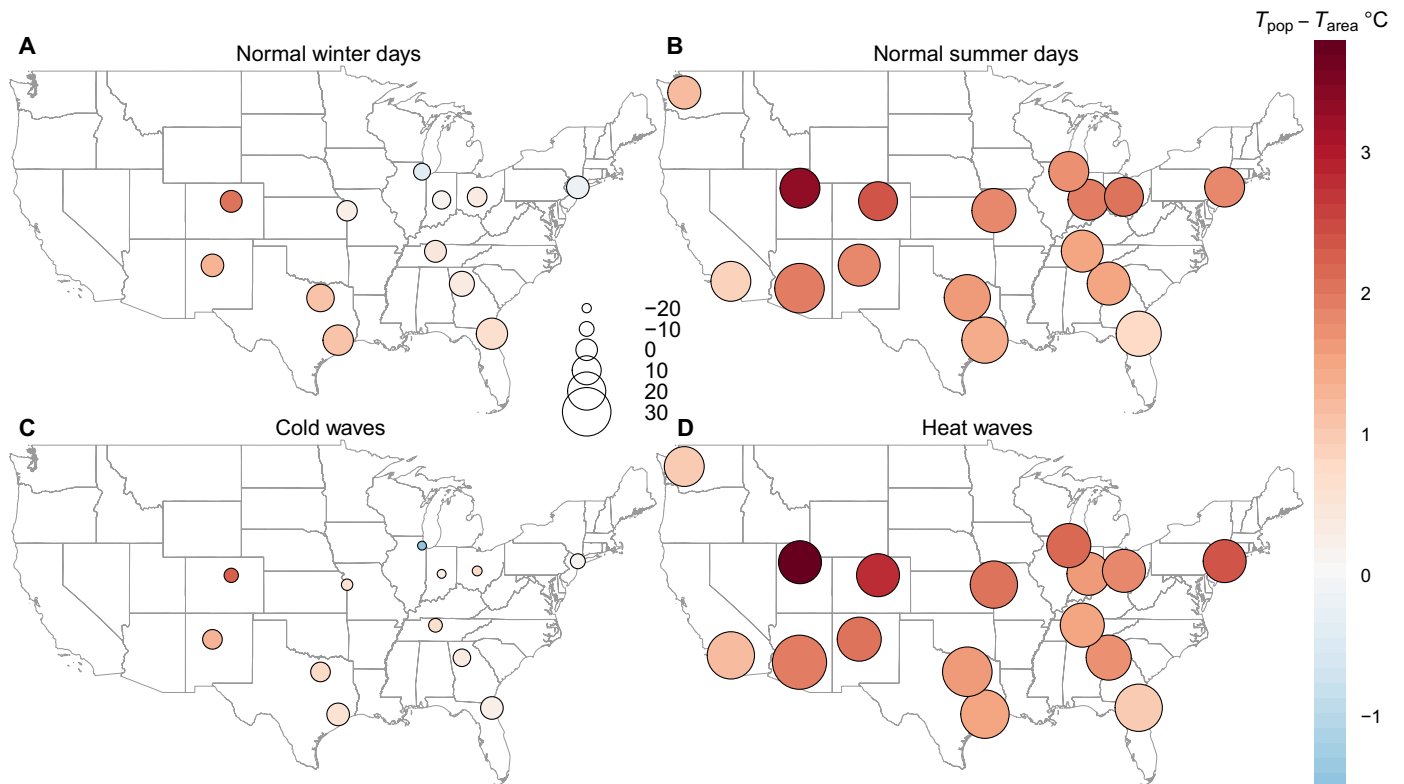

Fig. 1. Population dynamics–induced changes in residents' exposure temperature (T_{pop}– T_{area}) during simulated extreme events. (**A**) In normal winter days and (**C**) during the 2014 cold wave. (**B**) In normal summer days and (**D**) during the three simulated heat waves in 2006, 2011, and 2012. Each circle represents a metropolitan area affected by the extreme event, and its size is proportional to the magnitude of exposure temperature averaged over the entire metropolitan area without population dynamics (*Tarea*). The magnitude of changes for individual cities is referred to table S2.
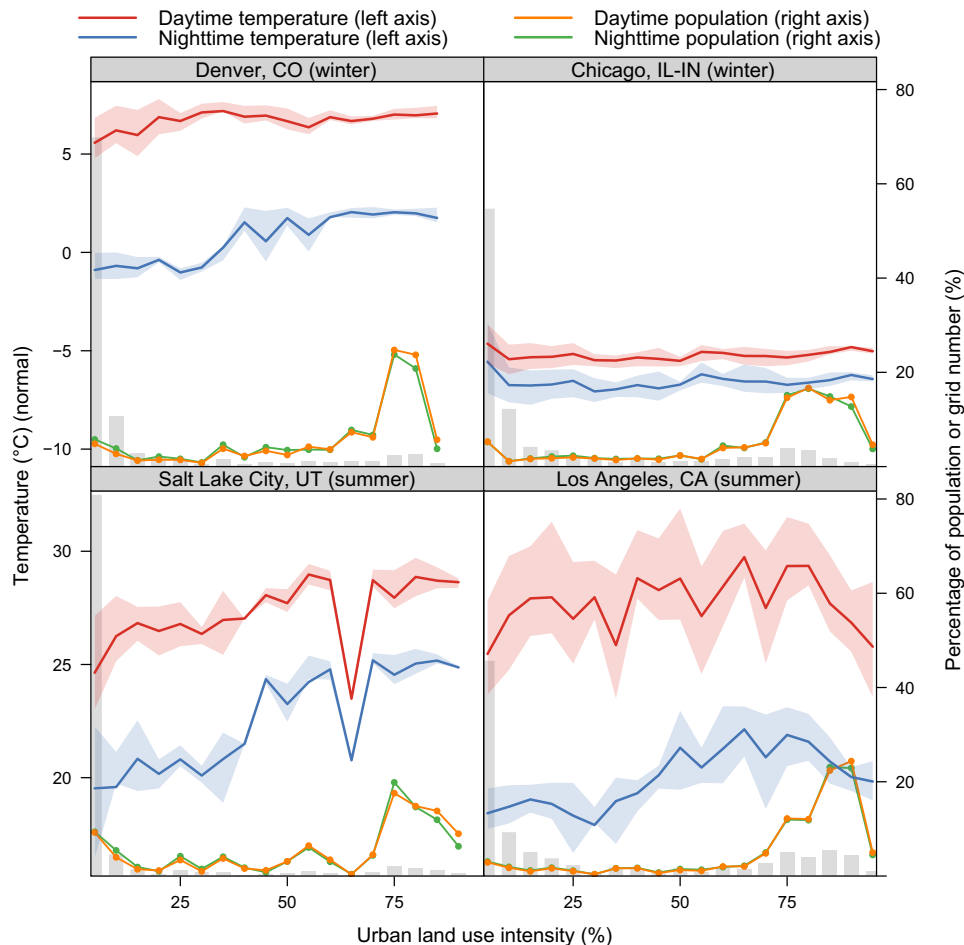
Fig. 2. Temperature, population, and grid number distributions as a function of urban land use intensity. Each gray bar stands for the percentage of grids within a 5% urban land use intensity interval to the total number of grids within the studied metropolitan area (right-side axis). Orange and green lines denote the ratios of population within grids of different urban land use intensities to the total population of the metropolitan area (right-side axis) at day and night. Shaded areas around the daily average temperature profiles (blue and red lines) stand for the 25% and 75% quantiles over grids within a 5% urban land use intensity interval (left-side axis).

temperatures over each metropolitan area. Within the domain, grids with low urban land use intensities dominate (large gray bars near the left side in Fig. 2), and the exposure temperature estimates without population dynamics (T_{area}) are largely determined by the temperature over less developed regions. On the other hand, population distribution profiles peak over high urban land use intensity areas (color lines in Fig. 2), and consequently, T_{pop} estimates are controlled by highly urbanized regions of the metropolis. Cities tend to have higher temperatures than their rural counterparts, known as the urban heat island effect, which suggests a positive relation between urban land use intensity and air temperature. During the cold wave, this positive relation (see Denver as an example in Fig. 2) results in higher temperatures over populous parts of the city (figs. S2 and S3), and T_{pop} is greater than T_{area}. Among the studied cities, Chicago is the only city where the movement of population intensifies their exposure to extreme low temperature under the cold wave (lower T_{pop} than T_{area} in table S2). In particular, daytime (0600 to 1800 local standard time) and nighttime (1800 to 0600 local standard time) temperatures are relatively homogeneous across areas with different urban land use intensities (shaded lines in Fig. 2). Populous urban areas are not remarkably hotter than other regions in Chicago; therefore, the overall exposure temperature of residents decreases

slightly over the diurnal cycle after accounting for population dynamics. Under studied heat waves, strong heat islands make heavily populated areas hot spots within the metropolitan area; hence, overall residents' exposure temperature is augmented (Los Angeles and Salt Lake City in Fig. 2). It is straightforward that the spatial extent of studied domains, especially the inclusion of low-intensity grids, will affect the absolute impact of population dynamics on exposure temperature. When focusing on smaller and more urbanized areas, population dynamics' effect declines as the study domain becomes more similar to populous regions within cities (fig. S4). Our selected domains, nevertheless, correspond to the weather forecast zones for individual metropolitan areas used by the National Weather Service. The estimated change in exposure temperature is, therefore, the temperature difference between what residents are exposed to and what they expect on the basis of weather forecast.

Figure 3 shows that the magnitude of temperature anomaly during the cold wave is positively related to the mean temperature under normal conditions (statistically significant at 0.05 level), indicating that cities in colder regions are subject to more intense cold hazards. Conversely, metropolitan areas with lower normal temperatures tend to experience larger temperature increases during heat waves. Daytime and nighttime anomalies are of similar magnitudes,
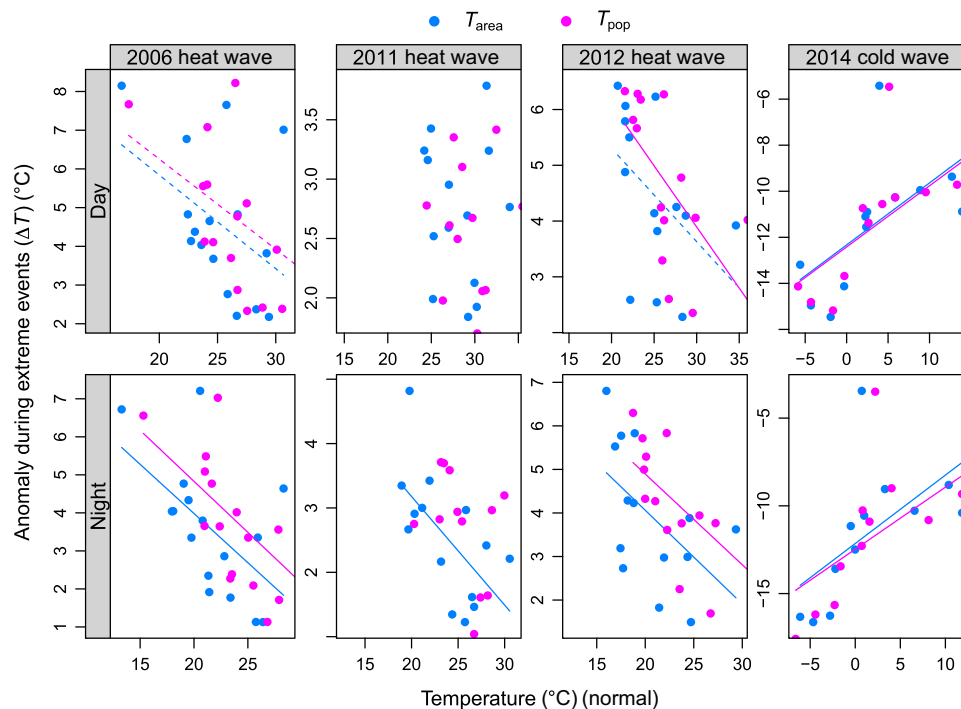
Fig. 3. Temperature anomalies over studied metropolitan areas during simulated extreme events. Solid (dashed) lines indicate the linear relationship is statistically significant at 0.05 (0.1) level.

but the trends are more statistically significant at nighttime. During the 2006 heat wave, the largest temperature anomaly of approximately 8°C in the coolest city is over three times greater than the 2°C anomaly found in the hottest city. This is worthy of special attention as residents in temperate climate are less prepared for extreme heat (*25*). We further investigate whether the impact of population dynamics on exposure temperature for extreme events and normal days is related to the cities' background climate, which contains temperature information in the long term. On the basis of the Köppen-Geiger climate classification, the relations are inconclusive for both heat and cold waves among studied cities (fig. S5).

Contributing factors for modified exposure

We now turn our attention to understanding how the variability of population and temperature and their interactions affect residents' exposure under extreme events. The spatial variability of temperature (see Materials and Methods) consistently shows a positive relation with population dynamics–induced changes in exposure temperature for three simulated extreme heat events (statistically significant at 0.05 level; Fig. 4A), while the spatial population variability shows a less significant relation (fig. S6A). Cities' spatial temperature variabilities are much smaller under heat waves than under the cold wave and fall within a narrow range. Under this circumstance, a small increase in the spatial temperature variability becomes important in affecting residents' heat exposure; thus, the effect of population dynamics correlates strongly with the spatial temperature variability. Unlike under extreme heat, cities respond to the extreme cold with a wide range of spatial temperature variability across the continent (Fig. 4A). The influence of spatial temperature variability therefore drops, and the reduced exposure of residents under extreme cold has a statistically significant relation with the spatial correlation of

temperature and population (Fig. 4B). Although the absolute impacts of population dynamics on residents' exposure temperature are small under extreme cold, the results highlight the benefit of anthropogenic warming for urban communities with high population density. Changes in the exposure temperature of urban residents have inconclusive relations with the spatial correlation of population and temperature under heat waves, yet we recognize that the effect of population dynamics is clearly larger at night than in daytime (fig. S6B).

DISCUSSION

The purpose of this study is to highlight the consistently overlooked impact of population dynamics on the exposure of urban residents to heat and cold waves. The modified exposure is caused by the daily commute of population through regions of different temperatures across the metropolitan area. Aggravated exposure of urban residents to extreme heat induced by intra-urban commute (1.9° ± 0.7°C) is more than half of the heat wave hazard (temperature anomaly of 3.6° ± 1.8°C), while the attenuated exposure to extreme cold (0.6° ± 0.8°C) is minor. Climate models project more frequent and more intense heat waves under the "business-as-usual" high greenhouse gas emissions. Analysis of climate extreme observations suggests more evident nocturnal warming than daytime warming during the past decades (*26*, *27*). In combination with the larger increases in exposure temperature induced by population dynamics at night (fig. S6), urban residents' adaptation to nocturnal extreme heat needs to be taken into serious consideration.

In the United States, the National Weather Service is responsible for issuing warnings for hazardous extreme weather. The current warning service released at the weather forecast zone level does not
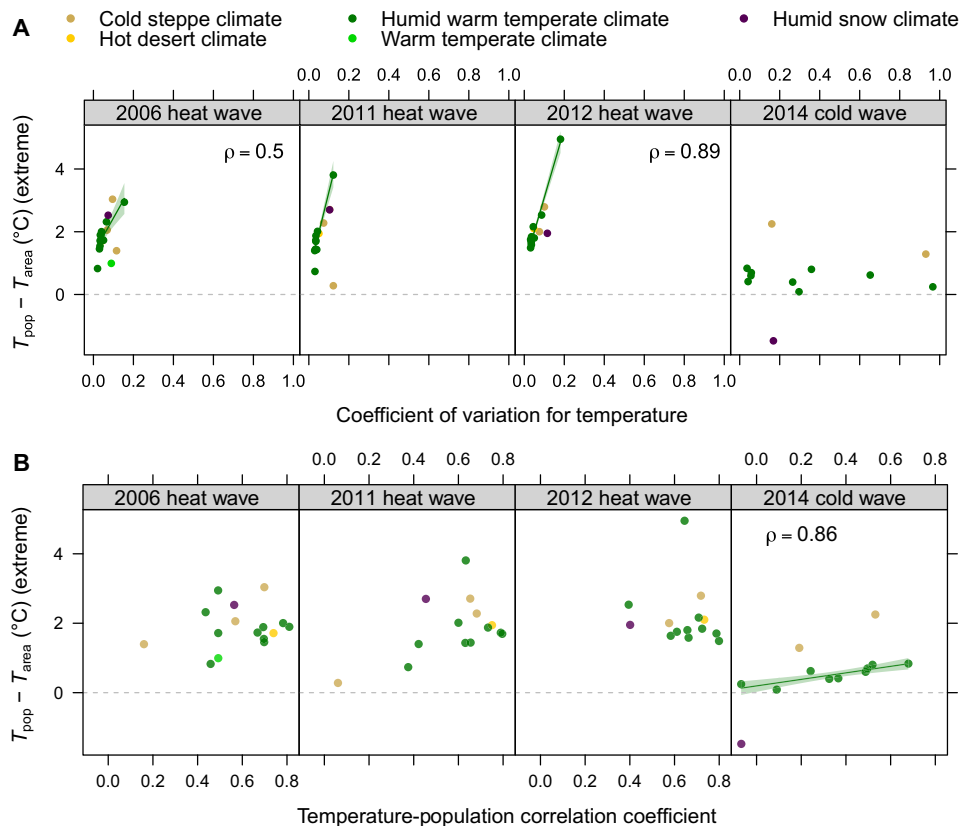
Fig. 4. The relations between population dynamics–induced changes in exposure temperature under extreme events and cities' temperature and population spatial variabilities. (**A**) Relations between the coefficient of spatial variation for daily average temperature over individual cities and the effect of population dynamics. (**B**) Relations between the effect of population dynamics and the spatial correlation coefficient of daily average temperature and population. The linear regression is performed for cities under the humid warm temperate climate with one standard deviation confidence band. Solid lines indicate the linear relation is statistically significant at 0.05 level.

consider spatiotemporal population dynamics; hence, its temperature forecast could deviate considerably from the exposure temperature of urban residents. These deviations can have severe consequences: False warnings lead to unnecessary actions of relevant agencies and a waste of public resources, while failure to capture extreme temperatures causes increased mortality and morbidity. Our approach in this study reduces the exposure bias of urban population at risk under extreme temperatures, and results reveal two important factors for modified exposure: the spatial temperature variability for heat wave and the temperature-population spatial covariation for cold wave. This finding reveals that residents' exposure to heat waves is more likely to be underestimated in a spread-out city, where the daily commute between residential areas and urban cores would induce a large change in the exposure temperature. The estimated risk based on the spatial average temperature performs poorly in large urban agglomerations, and the incorporation of population dynamics is essential for accurate characterizations of exposure temperature of urban residents in these regions. Existing heat mitigation/adaptation efforts have been mainly devoted to hot urban cores with high building densities (*28*), and these interventions are likely to be less efficient without considering residents' movement pattern. City planners and decision makers should identify the areas/paths of high population density to design climate adaptation strategies for reducing residents' exposure to extreme temperatures.

Two important limitations of this study need to be acknowledged. First, the weather-related stress and illness risk can be attributed to

multiple meteorological variables besides temperature, such as humidity, wind speed, and radiation (*29*), and the health outcome varies among population groups in different ages, socioeconomic statuses, and health conditions. Future analysis of resident exposure will benefit from the adoption of advanced indices more representative of human health and demographic status associated with the commuters. Second, the diurnal population flow in this study is estimated from the transportation census data and does not reflect the change from day to day. Population distribution is likely to change under extreme weather and subsequently modifies the exposure temperature of urban residents differently as compared to this study. A precise estimation of population dynamics requires the urban big data approach, which is not readily available at this stage.

MATERIALS AND METHODS
Definition of heat and cold waves
We collected daily mean 2-m air temperature (T_{mean}) data at weather stations in studied cities from the National Centers for Environmental Information (www.ncdc.noaa.gov/) for 1980–2010. Following the previous study (*6*), days with T_{mean} higher than the 95th percentile in warm seasons (May to September) are defined as heat waves, while days with T_{mean} lower than the 5th percentile of cool season (November to March) are defined as cold waves. We defined the normal days with T_{mean} between 10th and 90th percentiles for each

station. The classified periods through weather station measurements were applied to separate results during extreme events from normal days for numerical climate simulations described below.

Regional climate simulations

The advanced research version 3.8.1 of the Weather Research and Forecasting (WRF) model was adopted for carrying out weather simulations in this study. The WRF model is a powerful numerical tool with successful applications over major metropolitan areas worldwide (30). One single simulation domain was used to cover the entire United States with a horizontal resolution of 5 km. A set of well-tested physical parameterizations was used (31), including the rapid radiative transfer model for longwave radiation, the Dudhia shortwave radiation scheme, the Yonsei University planetary boundary layer scheme, and the Grell three-dimensional ensemble cumulus scheme. Initial and boundary condition data were obtained from the North American Regional Reanalysis by the National Centers for Environmental Prediction (https://rda.ucar.edu/datasets/ds608.0/). The selection of extreme events for this study was based on the spatial span of extreme events over the CONUS. We ran the hourly simulations for at least 30 days for individual study events, containing three major heat waves (13 July to 29 August in 2006, 11 July to 10 August in 2011, and 18 June to 20 July in 2012) and one cold wave (1 January to 1 February in 2014).

Land use/land cover information was obtained from the 2011 National Land Cover Database (NLCD) at 270-m resolution. We used the mosaic approach to solve for eight land use categories at every WRF grid (32); hence, the simulated 2-m air temperatures (T_a) accounted for the subgrid land surface heterogeneity. For nonurban grids, the 2-m air temperature was estimated from the Noah land surface model. For urban grids, air temperature was weighted on the basis of nonurban and urban portions of the grid cell

$$T_a = f_{imp} T_{urb} + (1 - f_{imp}) T_{rul}$$

where f_{imp} is the impervious fraction of the 5-km grid retrieved from the 2011 NLCD, T_{urb} is the 2-m urban air temperature computed by the single-layer urban canopy model (33), and T_{rul} is the 2-m rural air temperature simulated from the Noah land surface model. The National Urban Database with Access Portal Tool dataset was used to accurately represent urban morphological parameters for studied metropolitan areas where available (34).

We evaluated the simulated 2-m air temperature against measurements from 137 ground-based weather stations in studied cities (www.ncdc.noaa.gov/). The number of urban and rural stations used for individual cities is summarized in table S4. Overall, the WRF simulations reasonably capture the urban temperature during studied events over individual cities, with the mean absolute error of 2.2°C (table S4).

Diurnal population estimation

We estimated the hourly population distribution by redistributing the worker population during working hours (with an assumption of 8-hour working time and 1-hour lunch break). Residential population data from the census best describe the nighttime population distribution. The worker commute information, including where people live and commute to and from, when leaving for work and travel time, was extracted from the 2006–2010 Census Transportation Planning Products (CTPP) (https://ctpp.transportation.org/) to characterize the daytime population flow in addition to the resi-

dential population (35). The CTPP data provide the bulk number of population flow in and out of a geographic zone within a time interval but do not contain adequate information on the mode of commuting (e.g., by subway or by car) or the exact path of urban travelers. The travel data were aggregated to a 1-hour frequency for consistency with the temperature data. The spatial scale of the traffic analysis zone (finer than the census tract scale) was initially calculated for the diurnal commuter-adjusted population distribution and then was aggregated to 5 km to match the resolution of WRF simulations. We considered all the weather forecast zones containing the selected 16 metropolitan regions for the commute adjustment (fig. S2).

Temperature and population variations

To quantify the spatial variability of temperature and population with two distinct scales, we used a dimensionless measure of dispersion, the coefficient of variation (cv). It is defined as the ratio of the SD (σ) to the absolute value of the mean ($|\mu|$). We estimated the spatial variability cv on the basis of the daily average of temperature and population

$$cv = \sigma / |\mu|$$

The covariation of temperature and population was measured by the Pearson pairwise correlation coefficient.

SUPPLEMENTARY MATERIALS

REFERENCES AND NOTES

1. M. M. Huynen, P. Martens, D. Schram, M. P. Weijenberg, A. E. Kunst, The impact of heat waves and cold spells on mortality rates in the Dutch population. *Environ. Health Perspect.* **109**, 463–470 (2001).
2. B. Revich, D. Shaposhnikov, Excess mortality during heat waves and cold spells in Moscow, Russia. *Occup. Environ. Med.* **65**, 691–696 (2008).
3. P. G. Dixon, D. M. Brommer, B. C. Hedquist, A. J. Kalkstein, G. B. Goodrich, J. C. Walter, C. C. Dickerson IV, S. J. Penny, R. S. Cerveny, Heat mortality versus cold mortality: A study of conflicting databases in the United States. *Bull. Am. Meteorol. Soc.* **86**, 937–944 (2005).
4. A. G. Barnett, S. Hajat, A. Gasparrini, J. Rocklöv, Cold and heat waves in the United States. *Environ. Res.* **112**, 218–224 (2012).
5. J. Berko, D. D. Ingram, S. Saha, J. D. Parker, *Deaths Attributed to Heat, Cold, and Other Weather Events in the United States, 2006–2010* (National Health Statistics Reports, 2014).
6. J. F. Bobb, R. D. Peng, M. L. Bell, F. Dominici, Heat-related mortality and adaptation to heat in the United States. *Environ. Health Perspect.* **122**, 811–816 (2014).
7. Intergovernmental Panel on Climate Change, *Managing the Risks of Extreme Events and Disasters to Advance Climate Change Adaptation: Special Report of the Intergovernmental Panel on Climate Change*, C. B. Field, V. Barros, T. F. Stocker, D. Qin, D. J. Dokken, K. L. Ebi, M. D. Mastrandrea, K. J. Mach, G.-K. Plattner, S. K. Allen, M. Tignor, P. M. Midgley, Eds. (Cambridge Univ. Press, 2012).

8. B. G. Anderson, M. L. Bell, Weather-related mortality: How heat, cold, and heat waves affect mortality in the United States. *Epidemiology* **20**, 205–213 (2009).

9. B. Armstrong, Models for the relationship between ambient temperature and daily mortality. *Epidemiology* **17**, 624–631 (2006).

10. M. A. McGeehin, M. Mirabelli, The potential impacts of climate variability and change on temperature-related morbidity and mortality in the United States. *Environ. Health Perspect.* **109**, 185–189 (2001).

11. C. Mora, B. Dousset, I. R. Caldwell, F. E. Powell, R. C. Geronimo, C. R. Bielecki, C. W. W. Counsell, B. S. Dietrich, E. T. Johnston, L. V. Louis, M. P. Lucas, M. M. McKenzie, A. G. Shea, H. Tseng, T. W. Giambelluca, L. R. Leon, E. Hawkins, C. Trauernicht, Global risk of deadly heat. *Nat. Clim. Chang.* **7**, 501–506 (2017).

12. G. A. Meehl, C. Tebaldi, More intense, more frequent, and longer lasting heat waves in the 21st century. *Science* **305**, 994–997 (2004).

13. A. S. Voorhees, N. Fann, C. Fulcher, P. Dolwick, B. Hubbell, B. Bierwagen, P. Morefield, Climate change-related temperature impacts on warm season heat mortality: A proof-of-concept methodology using BenMAP. *Environ. Sci. Technol.* **45**, 1450–1457 (2011).

14. G. B. Anderson, K. W. Oleson, B. Jones, R. D. Peng, Classifying heatwaves: Developing health-based models to predict high-mortality versus moderate United States heatwaves. *Clim. Change* **146**, 439–453 (2018).

15. S. C. Sheridan, A. J. Kalkstein, L. S. Kalkstein, Trends in heat-related mortality in the United States, 1975–2004. *Nat. Hazards* **50**, 145–160 (2009).

16. S. Grimmond, Urbanization and global environmental change: Local effects of urban warming. *Geogr. J.* **173**, 83–88 (2007).

17. J. Yang, E. Bou-Zeid, Should cities embrace their heat islands as shields from extreme cold? *J. Appl. Meteorol. Climatol.* **57**, 1309–1320 (2018).

18. D. Li, E. Bou-Zeid, Synergistic interactions between urban heat islands and heat waves: The impact in cities is larger than the sum of its parts. *J. Appl. Meteorol. Climatol.* **52**, 2051–2064 (2013).

19. K. W. Oleson, G. B. Anderson, B. Jones, S. A. McGinnis, B. Sanderson, Avoided climate impacts of urban and rural heat and cold waves over the U.S. using large climate model ensembles for RCP8.5 and RCP4.5. *Clim. Change* **146**, 377–392 (2018).

20. B. Jones, B. C. O'Neill, L. McDaniel, S. McGinnis, L. O. Mearns, C. Tebaldi, Future population exposure to US heat extremes. *Nat. Clim. Chang.* **5**, 652–655 (2015).

21. M. Medina-Ramón, J. Schwartz, Temperature, temperature extremes, and mortality: A study of acclimatisation and effect modification in 50 US cities. *Occup. Environ. Med.* **64**, 827–833 (2007).

22. B. McKenzie, W. Koerber, A. Fields, M. Benetsky, M. Rapino, Commuter-adjusted population estimates: ACS 2006-10 (Journey to Work and Migration Statistics Branch, US Census Bureau, 2010).

23. W. Ma, L. Wang, H. Lin, T. Liu, Y. Zhang, S. Rutherford, Y. Luo, W. Zeng, Y. Zhang, X. Wang, X. Gu, C. Chu, J. Xiao, M. Zhou, The temperature–mortality relationship in China: An analysis from 66 Chinese communities. *Environ. Res.* **137**, 72–77 (2015).

24. L. Hu, O. V. Wilhelmi, C. Uejio, Assessment of heat exposure in cities: Combining the dynamics of temperature and population. *Sci. Total Environ.* **655**, 1–12 (2019).

25. R. S. Kovats, S. Hajat, Heat stress and public health: A critical review. *Annu. Rev. Public Health* **29**, 41–55 (2008).

26. L. V. Alexander, X. Zhang, T. C. Peterson, J. Caesar, B. Gleason, A. M. G. Klein Tank, M. Haylock, D. Collins, B. Trewin, F. Rahimzadeh, A. Tagipour, K. Rupa Kumar, J. Revadekar, G. Griffiths, L. Vincent, D. B. Stephenson, J. Burn, E. Aguilar, M. Brunet, M. Taylor, M. New, P. Zhai, M. Rusticucci, J. L. Vazquez-Aguirre, Global observed changes in daily climate extremes of temperature and precipitation. *J. Geophys. Res. Atmos.* **111**, D05109 (2006).

27. L. A. Vincent, T. C. Peterson, V. R. Barros, M. B. Marino, M. Rusticucci, G. Carrasco, E. Ramirez, L. M. Alves, T. Ambrizzi, M. A. Berlato, A. M. Grimm, J. A. Marengo, L. Molion, D. F. Moncunill, E. Rebello, Y. M. T. Anunciação, J. Quintana, J. L. Santos, J. Baez, G. Coronel, J. Garcia, I. Trebejo, M. Bidegain, M. R. Haylock, D. Karoly, Observed trends in indices of daily temperature extremes in South America 1960–2000. *J. Climate* **18**, 5011–5023 (2005).

28. E. S. Krayenhoff, M. Moustaoui, A. M. Broadbent, V. Gupta, M. Georgescu, Diurnal interaction between urban expansion, climate change and adaptation in US cities. *Nat. Clim. Chang.* **8**, 1097–1103 (2018).

29. S. Coccolo, J. Kämpf, J.-L. Scartezzini, D. Pearlmutter, Outdoor human comfort and thermal stress: A comprehensive review on models and standards. *Urban Clim.* **18**, 33–57 (2016).

30. F. Chen, H. Kusaka, R. Bornstein, J. Ching, C. S. B. Grimmond, S. Grossman-Clarke, T. Loridan, K. W. Manning, A. Martilli, S. Miao, D. Sailor, F. P. Salamanca, H. Taha, M. Tewari, X. Wang, A. A. Wyszogrodzki, C. Zhang, The integrated WRF/urban modelling system: Development, evaluation, and applications to urban environmental problems. *Int. J. Climatol.* **31**, 273–288 (2011).

31. M. Wang, M. Wagner, G. Miguez-Macho, Y. Kamarianakis, A. Mahalov, M. Moustaoui, J. Miller, A. VanLoocke, J. E. Bagley, C. J. Bernacchi, M. Georgescu, On the long-term hydroclimatic sustainability of perennial bioenergy crop expansion over the United States. *J. Climate* **30**, 2535–2557 (2017).

32. D. Li, E. Bou-Zeid, M. Barlage, F. Chen, J. A. Smith, Development and evaluation of a mosaic approach in the WRF-Noah framework. *J. Geophys. Res. Atmos.* **118**, 11918–11935 (2013).

33. J. Yang, Z.-H. Wang, F. Chen, S. Miao, M. Tewari, J. A. Voogt, S. Myint, Enhancing hydrologic modelling in the coupled Weather Research and Forecasting—Urban modelling system. *Boundary Layer Meteorol.* **155**, 87–109 (2015).

34. J. Ching, M. Brown, S. Burian, F. Chen, R. Cionco, A. Hanna, T. Hultgren, T. McPherson, D. Sailor, H. Taha, D. Williams, National urban database and access portal tool. *Bull. Am. Meteorol. Soc.* **90**, 1157–1168 (2009).

35. T. Kobayashi, R. M. Medina, T. J. Cova, Visualizing diurnal population change in urban areas for emergency management. *Prof. Geogr.* **63**, 113–130 (2011).